Published in final edited form as:
Toxicol Lett. 2014 August 17; 229(1): 198–209. doi:10.1016/j.toxlet.2014.06.009.

Single-walled carbon nanotube exposure induces membrane rearrangement and suppression of receptor-mediated signalling pathways in model mast cells

Eric Y. Umemoto, PhD.[1], **Mark Speck, PhD**[1], **Lori M.N. Shimoda, BS.**[1], **Kara Kahue, BS**[1,2], **Carl Sung, BS.**[1], **Alexander J. Stokes, PhD.**[3], and **Helen Turner, PhD.**[1,3]

[1]Laboratory of Immunology and Signal Transduction, Division of Natural Sciences and Mathematics, Chaminade University, Honolulu, HI

[2]Undergraduate Program in Computer Sciences, Division of Natural Sciences and Mathematics, Chaminade University, Honolulu, HI

[3]Department of Cell and Molecular Biology, John A. Burns School of Medicine, University of Hawaii, Honolulu, HI

Abstract

Carbon nanotubes (CNT) are environmental challenges to the respiratory and gastrointestinal mucosa, and to the dermal immune system. Mast cells (MC) are pro-inflammatory immunocytes that reside at these interfaces with the environment. Mast cells are sources of pro-inflammatory mediators (histamine, serotonin, matrix-active proteases, eicosanoids, prostanoids, cytokines and chemokines), which are released in a calcium-dependent manner following immunological challenge or physico-chemical stimulation. Since C-60 fullerenes, which share geometry with CNT, are suppressive of mast cell-driven inflammatory responses, we explored the effects of unmodified SWCNT aggregates on mast cell signaling pathways, phenotype and pro-inflammatory function. We noted SWCNT suppression of antigen-induced signalling pathways and pro-inflammatory degranulation responses. Mast cells recognize unmodified SWCNT by remodeling the plasma membrane, disaggregating the cortical actin cytoskeleton and relocalizing clathrin. Clathrin was also identified as a component of an affinity-purified ‘interactome’ isolated from MC using an SWCNT affinity matrix for mast cell lysates. Together these data are consistent with the ability of SWCNT to suppress mast cell pro-inflammatory function via a novel recognition mechanism.

Corresponding author. Helen Turner, Ph.D., Professor of Biology, Chaminade University, 3140 Waialae Avenue, WSC 116, Honolulu, Hawaii, 96816, hturner@chaminade.edu, phone: 1 (808) 778 8920, Fax: 1 (808) 440 4278.

Author Contributions. EU, MS, KK, LS and CS performed experiments and analyses. EU, MS, AJS and HT wrote the manuscript.

Keywords

Carbon nanotubes; fullerenes; mast cells; inflammation

1. Introduction

The interaction between biomolecules and nanoreagents has been identified as having the potential to yield new nanomaterials with unique properties (Ajayan et al., 1999; Battigelli et al., 2013; Bianco et al., 2005). Humans are beginning an era of unprecedented level of interaction with nanomaterials derived from elemental carbon (carbon nanotubes, CNT). Both the single-walled (SWCNT) and multiwalled (MWCNT) carbon nanotubes display unique mechanical, chemical and electrical properties that can be further modified or functionalized with additions of various side chain moieties (Battigelli et al., 2013; Bianco et al., 2005; Cui et al., 2012). The ability to modify CNTs have further increased their utility and made them compelling candidates for delivery of nano-therapeutics

While the applications for nanotechnology seem endless, the impact of their use environmentally and clinically has raised both safety concerns as well as a need for consistent methodologies to evaluate their safety (Ajayan et al., 1999; Firme and Bandaru, 2010; Stern and McNeil, 2008). Whether humans are exposed to CNTs directly as with drug delivery or indirectly through the use in the environment, these materials may represent novel challenges to the respiratory and GI mucosa, and to the dermal immune system (Ajayan et al., 1999; Firme and Bandaru, 2010; Stern and McNeil, 2008). The mast cell is a pluripotent, pro-inflammatory immunocyte that resides at these sites in the body. Mast cells release pro-inflammatory mediators (including histamine, serotonin, matrix-active proteases, bioactive eicosanoids and prostanoids, cytokines and chemokines) in response to immunological and physico-chemical stimuli (Galli and Tsai, 2010; Marshall, 2004; Moon et al., 2010; Sismanopoulos et al., 2012).

Mast cells respond to a wide array of stimuli, including challenges to adaptive and innate immunity, physical inputs (heat, pH) and biochemical stimuli (cytokines, growth factors, hormones and neurotransmitters) (Galli and Tsai, 2010; Marshall, 2004; Moon et al., 2010; Sismanopoulos et al., 2012). The ability to recognize simple repeated-pattern biomolecules is common to various immunocytes including mast cells, which bear innate receptors for collagens, and other extracellular matrix proteins, Pathogen- and Danger-associated molecular patterns (PAMPs and DAMPs) such as nucleic acids and DAMPs such as heparan and uric acid (Galli and Tsai, 2010; Koyasu and Moro, 2012; Sandig and Bulfone-Paus, 2012). Thus mast cells couple the perception of structurally simple environmental challenges to inflammatory responses.

There is little extant literature on CNT and mast cells, with most studies having focused upon the phagocytic macrophage and various lymphocytes. However, a 2007 study examined the effect of functionalized polyhydroxy C-60 and N-ethyl-polyamino C-60 CNTs on systemic and cutaneous anaphylactic responses, which are primarily mediated by histamines, vasoactive peptides and other pro-inflammatory mediators released from mast cells. These data suggest that fullerene compounds are markedly anti-inflammatory *in vivo*,

via suppression of mast cell-mediated responses. These data create the need to first assess whether CNT, which share elements of the fullerene geometry, are similarly anti-inflammatory (Ryan et al., 2007). This is a possibility that would seem paradoxical since CNT are widely regarded as having the capacity to initiate macrophage-based inflammation and act pro-fibrotically (Ali-Boucetta et al., 2013; Firme and Bandaru, 2010; Murphy et al., 2012; Murray et al., 2009; Poland et al., 2008). Second, both CNT and fullerenes need to be assessed for their ability to directly interface with mast cells and identify any cognate receptors that are involved.

In this study we explored the effects of unmodified SWCNT aggregates on mast cell signaling pathways, phenotype and pro-inflammatory function. We noted suppression of antigen-induced signalling pathways and pro-inflammatory degranulation responses when exposed to unmodified SWCNT. In addition to looking at effects on function, we tested the ability of mast cells to recognize the basic structures formed by unmodified SWCNT. Confocal microscopy was used to create three-dimensional reconstructions of the remodeled plasma membrane around SWCNT aggregates. Consistent with this plasma membrane remodeling, staining of cortical actin revealed disruption of the cytoskeleton in the contact zone between the plasma membrane and SWCNT. Identification of possible interactions between SWCNT and mast cell proteins were identified by analysis of the proteins purified when unmodified SWCNT were used as an affinity matrix. When compared with controls, several components of the clathrin internalization complex were over-represented. Additional staining revealed clustering of clathrin at or near the contact point of the plasma membrane and SWCNT. Together these data are consistent with the ability SWCNT to suppress mast cell pro-inflammatory function via a previously uncharacterized recognition mechanism.

2. Materials and Methods

2.1. Cell culture

RBL2H3 (Passante and Frankish, 2009) were grown at 37 °C, 5% CO_2, in 95% humidity in DMEM (containing ∼10μg/ml Fe) /10% heat-inactivated FBS /2mM Glutamine.

2.2. Chemicals, Antibodies

General chemicals were from VWR (West Chester, PA) and Sigma (St. Louis, MO). Phorbol 12,13-myristate acetate (PMA) and ionomycin were from Calbiochem (Gibbstown, NJ). Antibodies were sourced as follows: phospho-p72syk, phospho-ERK1/2, phospho-AKT (Ser 473) were from Cell Signaling Technologies (Danvers, MA). Anti-phospho-phospholipase C gamma 1 was from BD Biosciences (San Jose, CA). Anti-phospho-NFATC1 (Ser54) and anti-clathrin were from Abcam (Cambridge, MA). Anti-Grb2 was from Upstate Biotechnologies (Billerica, MA). Alexa-conjugated wheat germ agglutinin (WGA), Alexa- and HRP conjugated secondary antibodies were from Invitrogen (Temecula, CA) and Amersham (Piscataway, NJ).

Water-soluble hydroxylated fullerene derivatives ($C_{60}(OH)_n$, polyhydroxy C-60 modified with 18-22 hydroxyls) were obtained from BuckyUSA (Houston, TX). SWCNT were produced by CVD at >95% purity and <5% Fe contamination (Nano-Labs, Detroit, MI).

Note that DMEM contains ~0.0001g/L $FeNO_3.9H_2O$. TEM shows a SWCNT width range of 10-21 nm and a mixture of agglomerated and single SWCNT with lengths ranging from <2 to >10 microns. Measured aggregate sizes interacting with cells ranged from ~100nm to >1 micron diameter. Doses of SWCNT from 10-100 μg/ml were calculated to equate to 2.8-28 micrograms per cm^2 in microscopy applications.

2.3. Affinity Purification and MALDI-MS

Single walled carbon nanotubes (SWCNT, 10 μg) were incubated with Tx-100 lysates (see below) from 10 million RBL2H3 in triplicate. Lysis buffer alone and an irrelevant matrix (marine collagen) were used in parallel. Affinity purifications proceeded at 4°C with rotation for 2h, and then the matrices were washed 6 times in lysis buffer. Tryptase digestion was performed on the matrix, without elution, and multidimensional protein identification technology (MuDPIT) using 2D LC coupled to MS/MS was performed at the Keck Biotechnology Resource Laboratory, Yale University.

Cell Stimulations—FcεRI stimulation used 0.1μg/ml IgE anti-dinitrophenol (DNP, 16 h/ 37°C) (Sigma) followed by three washes and the addition of 250ng/ml keyhole limpet hemocyanin (KLH) conjugated-dinitrophenol (DNP, Calbiochem) for indicated times. Phorbol 12, 13 myristate acetate (PMA) and ionomycin were both used at 500nM.

Cell Lysis and Western blot—10^7 cells were lysed (ice/30 minutes) in 350μl of lysis buffer (50mM Hepes pH 7.4, 250mM or 75mM (high and low salt, respectively) NaCl, 20mM NaF, 10mM iodoacetamide, 0.5%(w/v) Triton X100, 1mM PMSF (phenylmethylsulfonylfluoride), 500 μg/ml aprotinin, 1.0 mg/ml leupeptin and 2.0 mg/ml chymostatin). Lysates were clarified (17,000*g*, 20 min), acetone precipitated (1.4 volumes acetone for 1h at −20°C, and centrifuged (10,000*g* for 5 min) and resolved by 10% reducing SDS-PAGE. Resolved proteins were electro-transferred to PVDF in 192mM glycine, 25mM Tris (pH 8.8). For Western blotting, membranes were blocked using 5% non-fat milk in PBS for 1 hour at RT. Primary antibodies in PBS/0.05% Tween-20/0.05% NaN_3 were incubated for 16 hours/4°C. Developing antibodies comprised anti-rabbit or anti-mouse IgGs conjugated to horseradish peroxidase (Amersham) diluted to 0.1μg/ml in PBS/0.05% Tween-20 and incubated with membranes for 45 minutes at RT. Four 5 min washes separated each step. Signal was visualized using enhanced chemiluminescence (Amersham) and exposure to Kodak BioMax film. Quantification was performed using NIH Image J.

2.4. Immunocytochemistry

Cells were fixed with 0.4% (w/v) paraformaldehyde (1h, RT), washed twice with dH_2O and stained sequentially with primary and secondary (Alexa Fluor IgG with indicated fluorophores) antibodies dissolved in PBS/0.75$ FSG. Three washes in PBS were performed after each step. Coverslips were mounted in Crystal-Mount (Electron Microscopy Sciences, Hatfield, PA). Bright field and fluorescence imaging were performed on a Nikon Ti Eclipse C1 epi-fluorescence and confocal microscopy system, Images were analysed in NIS Elements (Nikon, Melville, NY). Unless otherwise stated images were acquired through a Plan Apo VC 100× 1.40 oil objective (Nikon).

2.5. Calcium assay

RBL2H3 were washed and incubated with 1μM Fluo-4 AM, for 30 minutes at 37°C in a standard modified Ringer's solution of the following composition (in mM): NaCl 145, KCl 2.8, CsCl 10, $CaCl_2$ 2 (or 0), $MgCl_2$ 2, glucose 10, Hepes·NaOH 10, pH 7.4, 330 mOsm. For nominally calcium free experiments 1mM EGTA was added to the external solution and calcium chloride was omitted. Cells were transferred to 96-well plates at 50 000 cells/well and stimulated as indicated. Calcium signals were acquired using a Flexstation 3 (Molecular Devices, Sunnydale, USA). Data were analyzed using SoftMax® Pro 5 (Molecular Devices).

2.6. Beta-hexoseaminidase assay

RBL2H3 were plated in cluster plates at 5×10^4 cells/well. Monolayers were washed and incubated in 200 μl Tyrode's buffer before stimulating as described. After 45 min at 37°C, 25 μl supernatant was removed, clarified by microcentrifugation, and transferred to a 96 well plate containing 100 μl per well 1 mM *p*-N-acetyl glucosamine (Sigma) in 0.05 M citrate buffer pH 4.5. After 1 h at 37°C reactions were quenched by the addition of 100 μl per well 0.2 M glycine, pH 9.0. Beta-hexoseaminidase levels were read as OD at 405 nm.

2.7. Electron Microscopy

Cell pellets were stained in 1% osmium tetroxide (PBS) for 45 min at RT (diluted in PBS). Pellets were rinsed with PBS 3× for 10 min. Pellets were serially dehydrated (50% ethanol/10 min, 70% ethanol/10min/3. Pellets were moved to BEEM capsules and 1:1 dilution of 100% ethanol and resin was added and left for 1 hour. This was removed and 100% resin was added and samples vacuum oven cured for 16h. Samples were sectioned using a Leica ultramicrotome to 70nm sections and placed on formvar carbon coated copper grids. The samples were imaged on a Hitachi H7800 at magnifications ranging from 3,000×-300,000×.

2.8. Analysis

Results are shown as the mean + standard deviation. Statistical significance was determined based on ANOVA or A Student's t-test. Adjacent to data points in the respective graphs, significant differences were recorded as follows: single asterisk, $p < 0.05$; double asterisk, $p < 0.01$; triple asterisk, $p < 0.001$; no symbol, $p > 0.05$. Experiments are all *n* of at least 3.

3. Results

3.1. SWCNT are recognized by model mast cells

Tissue-resident mast cells respond to a plethora of inputs, including physical, chemical and biological stimuli. Situated at the body's interfaces with the environment, these cells respond to a variety of simple biological macromolecules, such as extracellular matrix components and the pattern and danger associated molecular patterns (Galli and Tsai, 2010). Mast cell responsiveness to macromolecules with fullerene geometry has previously been suggested by *in vivo* work (Ryan et al., 2007), and we asked if a model mast cell line amenable to *in vitro* studies supported the idea that these cells directly sense and respond to carbon nanotubes.

Single walled CNT (SWCNT) were selected for this study, and applied to cells following centrifugation (1,000*g*) that removed large aggregates but contained both dispersed (150 nm length) and particulate aggregates up to 2 microns in diameter. We reasoned that environmental exposures to CNT might well take this mixed form, and that dispersal agents could confound signalling outcomes. Moreover, initial experiments were performed with both unfractionated and 10,000*g* supernatants (the later having no >0.5 micron aggregates upon microscopic inspection) and no differences in experimental outcome were noted.

We asked if model mast cells contained proteins that could be affinity purified using SWCNT as a matrix. RBL2H3, a rat basophilic cell line with phenotypic features of mucosal mast cells (Passante and Frankish, 2009), were lysed and incubated with SWCNT as an affinity matrix, and an irrelevant matrix control. MUDPIT analysis with 2D LC coupled to MS/MS revealed a set of approximately 27,000 peptides, which we collapsed to a set of 400 proteins, of which 96 were represented multiply. We assessed the remaining proteins and identified which were over represented by at least threefold in terms of peptide abundance in SWCNT affinity purifications compared to an irrelevant marine collagen matrix. Those peptides are identified in Figure 1, with their relative (%) distribution in distinct canonical groups and gene names. This data set is likely to represent both direct and indirect interacting partner proteins for SWCNT.

The relatively large number of proteins found to associate with the SWCNT led us to seek a complementary method for identifying potential direct interactors. In Figure 1B we analysed the chemical characteristics of 34 peptides that have been suggested in the literature as potentially binding to CNT (Cui et al., 2010; Li et al., 2006). We sought to identify common features that could then be used to interrogate our protein interactor library. Some of the most obvious features of this analysis are histidine (basic) and aromatic hydrophobic character over-representation. Several instances were noted where peptides that have the charge characteristics (His-rich) to presumably form non-covalent interactions with CNT surfaces also contain the Tyr-Arg-X motif associated with interaction with the Clathrin AP1/2 proteins, both of which were present in our affinity purification set (Boll et al., 1996; Ohno et al., 1995). Interestingly, the first 10 amino acids of human Chain A, AP2 contain 6 histidines (GI 10120836).

Several components of the clathrin internalization complex were over-represented in the SWCNT affinity purifications relative to controls. Western blot analysis for clathrin in affinity purifications was inconclusive, and we therefore sought to assess the subcellular localization of clathrin under conditions of SWCNT exposure. Figure 2A shows the subcellular localization of anti-clathrin immunofluorescence in resting and SWCNT-exposed mast cells. Relocation of punctate clathrin complexes towards the plasma membrane was noted within 10 min of SWCNT exposure and measured using intensity line scan analysis (Figure 2B). Both microscopically (not shown) and by Western blot (Figure 2C), we note that total cellular clathrin levels diminished with long time-courses of exposure to SWCNT (1h or greater). Taken together, these data suggest that the clathrin internalization complex may be a component of the cellular recognition and response to SWCNT (Pauly and Drubin, 2007; Yaron et al., 2011).

We asked if larger particulate SWCNT aggregates were recognized by model mast cells. While no clathrin redistribution more pronounced than that shown in Figure 2B was noted (not shown) we did observe that large SWCNT aggregates caused striking membrane rearrangements in these cells. Figure 3A-D show a representative cell stained with Alexa 488-WGA to visualize the cell membrane, interacting with a ∼1 micron diameter SWCNT aggregate 2 min after exposure. Three dimensional reconstructions visualized either as reconstructed 180nm z stacks (A, B) or z-depth coded extended depth of focus images (C) suggest that the large SWCNT aggregates (examined by EM in Figure 3D) cause marked membrane perturbation, with the membrane moulding around the aggregate in a rapid and reversible manner. This remodelling is associated with disruption of the cortical actin cytoskeleton. Figure 3E-H present analysis of fluorescently labeled phalloidin distribution in a cell exposed for 2 min to an SWCNT aggregate. Compared to areas of the cell not in contact with the SWCNT aggregate, the contact zone between cell and aggregate is marked by apparent fragmentation and disruption of the cortical actin cytoskeleton. Taken together, these data suggest that interaction with either dispersed or aggregated SWCNT causes marked alterations in the morphology of model mast cells.

3.2 SWCNT exposure suppresses degranulation in model mast cells

The data presented above suggest altered membrane structure and actin cytoskeleton disruption in SWCNT-exposed mast cells. Moreover, mast cell dependent anaphylactic responses are suppressed in mice systemically injected with C-60 fullerene compounds (Ryan et al., 2007). We asked whether CNT, which are different forms of the fullerene geometry, can also suppress mast cell pro-inflammatory responses, and used an in vitro assay system to establish whether this suppression might represent a direct effect of CNT exposure on mast cell activation.

Figure 4 examines immunologically and pharmacologically induced RBL2H3 degranulation responses in the absence and presence of SWCNT. Both acute (30 min-4h), and chronic (1-4d), incubation with SWCNT result in significant ($p<0.05$) suppression of degranulation responses induced by antigenic cross-linking of the high affinity receptor for IgE (FcεRI) (Figure 4A and B).

3.3. SWCNT exposure suppresses calcium mobilization in model mast cells

Activation of mast cells via their primary antigen receptor, FcεRI, is absolutely dependent upon a biphasic mobilization of intracellular free calcium levels. Ins (1,4,5) O3-mediated depletion of intracellular calcium stores is directly coupled to calcium influx across the plasma membrane via channels of the store-operated ORAi family (Di Capite and Parekh, 2009; Ma and Beaven, 2011). We hypothesized that suppression of degranulation responses, a calcium dependent process, could reflect SWCNT interference with calcium signalling pathways. Figure 5A shows that antigen-induced calcium responses, measured via Fluo-4, are suppressed by chronic (1-6d) incubation of cells with 10μg/ml suspensions of SWCNT. Pharmacologically-induced calcium responses (using the ionophore ionomycin) are also suppressed, suggesting that SWCNT exposure affects common elements of the calcium entry pathway. Doses of SWCNT as low as 100ng/ml SWCNT can inhibit FcεRI-induced calcium responses to a statistically significant degree (Figure 5B). Moreover, the

suppressive effects of SWCNT on antigen-induced calcium responses are apparent within 30 min of SWCNT exposure (Figure 5C). Experiments performed in the presence and absence of external calcium show that CNT exposure suppresses both the influx and the store depletion phases of an antigen receptor induced calcium signal (Figure 5D-F). Since there are cell cycle-associated effects on calcium signalling, we assessed whether there are growth effects of SWCNT exposure in these cells. Figure 5G shows that no alteration in cellular proliferation is apparent over a 5d period of SWCNT exposure. Taken together, these data indicate that a component of the suppressive effects of SWCNT exposure on mast cell degranulation may be attributable to compromised calcium responses.

3.4. Altered activation of FcεRI-regulated signalling pathways following SWCNT exposure

Functional responses in mast cell depend on activation of membrane-proximal and cytoplasmic kinase signalling pathways. We asked if SWCNT exposure altered activation of these pathways. Figure 6A shows that incubation with SWCNT suppresses FcεRI -induced phosphorylation of the syk kinase, PLCγ1, the ERK and AKT kinases (Figure 6A) and AMP kinases α and β (Figure 6B). Anti-phosphotyrosine Western analysis (Figure 6C) supports the idea that multiple kinase targets are less phosphorylated when antigenic crosslinking occurs in cells pre-exposed to SWCNT. These data suggest that kinase signaling pathways are compromised in SWCNT-treated cells, which may contribute to down-regulation of degranulation.

3.5. Hydroxylated fullerenes are suppressors of FcεRI pathways in vitro

SWCNT share fullerene geometry with carbon-60 ‘buckyballs’. Suspensions of C-60 have been shown to suppress mast cell-mediated hypersensitivity reaction *in vivo* (Ryan et al., 2007). Figure 7A shows that, in contrast with SWCNT, C60 fullerenes do appear to be internalized in RBL2H3. While we could not obtain evidence from EM studies (not shown) that SWCNT aggregates attained the cytoplasm (remaining aggregated in large clumps at the plasma membrane), C60 fullerenes could be noted in the cytoplasm and in discrete subcellular structures after as little as 10 min exposure. We used our *in vitro* assay system to assess whether the anti-inflammatory action of C-60 reported by Ryan *et al* could represents direct action upon mast cell signalling pathways. Figure 7A shows that both unmodified and hydroxylated C-60 suppress degranulation responses in RBL2H3. Similarly to the action of SWCNT, C-60 also suppress syk phosphorylation following antigenic cross-linking of FcεRI (Figure 7B).

4. Discussion

Fullerenes are allotropes of carbon that display unique mechanical and electrical properties. Their small size, inertness and ability to be functionalized and combined with therapeutic molecules have led to numerous proposed applications in drug and gene delivery (Ajayan et al., 1999; Battigelli et al., 2013; Bianco et al., 2005). Almost every technological field has been impacted by the potential applications of nanomaterials, making human exposure to these nanomaterials increasingly prevalent. These materials represent novel challenges to the respiratory and GI mucosa, and to the dermal immune system. In animal models, dermal exposure of CNTs has been shown to induce both acute and chronic inflammation causing

fibrosis (Ali-Boucetta et al., 2013; Murphy et al., 2012; Poland et al., 2008; Stern and McNeil, 2008). *In vivo*, distribution and function of CNTs are influenced by the method of delivery, length and functionalization. For example, long MWCNTs that are difficult for phagocytes to internalize can trigger chronic inflammation, granulomas and pathogenicity similar to asbestos fibers (Ali-Boucetta et al., 2013; Bianco et al., 2005; Murphy et al., 2012; Poland et al., 2008; Stern and McNeil, 2008).

Here, we show that acute and chronic exposure of model mast cells to non-functionalized SWCNT suppresses their pro-inflammatory response. This suppression was observed both as a reduction of the antigen induced calcium response as well as inhibition of the subsequent release of pro-inflammatory mediators. Mast cells incubated from 1 to 6 days with 10μg/ml of SWCNTs displayed larger reductions in antigen-induced calcium responses at 6 days than at 1 day. Calcium entry was highly sensitive to SWCNT, with significant inhibition either at short (<1h) timepoints and at low (ng/ml) concentrations. Moreover, both store release and calcium influx were inhibited by SWCNT exposure, suggesting that receptor mediated signalling pathways may be being targeted (Di Capite and Parekh, 2009; Ma and Beaven, 2011). Interestingly, calcium entry in response to ionophore, which is receptor independent, was also inhibited by SWCNT, which may reflect some level of blockade of cell surface calcium entry channels themselves. Overall, CNT exposure suppressed antigen-induced calcium entry in mast cells in a time- and dose-dependent manner. The signalling cascade that follows FcεRI stimulation in mast cells involves phosphorylation of multiple kinases. Western blot analysis showed incubation with SWCNT suppressed FcεRI-induced phosphorylation of multiple kinases in the cascade such as the syk, PLCγ1, the ERK and AKT. Thus even without functionalization, CNT exposure suppressed calcium responses and inhibited phosphorylation of kinases associated with antigen stimulation, suggesting that CNTs share with C-60 fullerenes the ability to suppress mast cell pro-inflammatory responses (Ryan et al., 2007).

A recent study by Katwa et al (2012) shows that mast cell deficient mice are effectively rescued from pulmonary and cardiovascular toxicity induced by MWCNT. These chronic exposures are likely inducing localized inflammation and fibrosis, both processes in which mast cells are thought to act as tissue-resident orchestrators. This suggests that, in a tissue context, with chronic exposure, MWCNT exposure is broadly pro-inflammatory, presumably driving the release of bioactive lipids, cytokines and matrix-active proteases from tissue-resident mast cells. Our current data, and those of Ryan et al, suggest that acute pro-inflammatory responses such as histamine release from mast cells can be directly suppressed by exposure to carbon nanomaterials. These are very different study designs and tissue systems, but we can conclude that if indeed exposure to CNT is acutely suppressive of mast cells responses, in the long term tissue damage may result from the chronic presence of the nanomaterials, with mast cells also contributing to this long term disruption of tissue status. Both studies are clearly of interest when considering the potential anti-inflammatory applications and side-effects of CNT-based therapeutics.

Additional changes caused by fullerenes could also contribute to suppression of mast cell activation. Immunochemical stains of poly C-60 and N-ethyl C-60 CNTs found that the CNT were internalized and localized in the cytoplasm (Dellinger et al., 2010). Ryan *et al*

further suggested the suppressive effects of fullerenes observed in mast cells could be partly explained by the ability of fullerenes to scavenge ROS (Ryan et al., 2007). Once in the cytoplasm the presence of fullerenes would reduce cellular levels of ROS and inhibit activation of subsequent pathways regulated by ROS. In RBL (the mast cell line used here), generation of ROS after antigen stimulation has been shown to have a role in degranulation and leukotriene release (Murray et al., 2009; Suzuki et al., 2009; Yoshimaru et al., 2002). In addition to the inhibition of antigen stimulated ROS mediated pathways, array data further suggested incubation with poly C-60 and N-ethyl C-60 CNTs also reduced syk phosphorylation (Ryan et al., 2007), which our study further supports.

A study of C-70 fullerenes conjugated with Texas Red in skin mast cells found that a majority of the fullerenes localized to the ER and to a lesser extent lysosomes and mitochondria (Dellinger et al., 2010). Coincident with this localization was a reduction of ROS production and calcium responses after FcεR1 stimulation. Although studies with mast cells are limited, our data using unmodified SWCNT aggregates and RBLs are consistent with groups that found similar suppression of pro-inflammatory and calcium responses after exposure to functionalized SWCNTs on human mast cells (Dellinger et al., 2010; Ryan et al., 2007).

Studies using different modifications of carbon nanomaterial highlight the relationship between localization of the carbon nanomaterial and its formulation. EM images suggest a basic difference between fullerenes, which were found internalized, and SWCNT that were found externally and in contact with the plasma membrane. This may highlight a difference in the ability of the model mast cell to recognize and internalize these particles. While additional experiments need to be performed to confirm that SWCNT are not being internalized at a level below our detection limits, these data support our view that SWCNT aggregates externally suppress mast cell responses.

Consistent therapeutic use will require a more specific understanding of both the mechanisms of internalization as well as subsequent localization. Numerous studies have demonstrated endocytosis/phagocytosis as the major pathway of internalization (Jin et al., 2009; Yaron et al., 2011). Chemical inhibitors of endocytosis such as filipin and amiloride prevented internalization of the Texas Red-modified CNTs in skin mast cells (Dellinger et al., 2010). Endocytosis can involve multiple pathways with both size of the particle and the ability for recognition influencing which pathways are utilized. Thus characterizing the affinities of SWCNTs to molecules in the plasma membrane could help predict how they are internalized.

Although we did not localize SWCNT internally (due to our commitment to using unmodified CNT without attached fluorophores), plasma membrane reorganization and remodeling of cortical actin at the interface of the SWCNT aggregates and the plasma membrane are consistent with the ability of mast cells to sense the presence of SWCNT in their environment. Three dimensional reconstructions of these interactions show the plasma membrane responding to the presence of SWCNT within minutes. To attempt to understand what molecules, if any, may recognize or interact with unmodified SWCNT, we used the CNTs as an affinity matrix to purify binding proteins from lysed RBL2H3. These data likely

included identification of molecules that are engaged in both direct and indirect interactions with SWCNT aggregates, as well as inevitable contamination with non-specific binding partners. Further analysis of the overrepresented interactions with CNT is required but we noted that clathrin and several components of the clathrin-mediated internalization complex were over-represented in the SWCNT binding set relative to an irrelevant control matrix.

The triskelion structure of clathrin is geodesic (Pauly and Drubin, 2007). Clathrin-mediated endocytosis is an entry mechanism for various environmental factors including bacteria, viruses and other particulates (Cureton et al., 2010; Pauly and Drubin, 2007; Pelkmans and Helenius, 2003; Piccinotti et al., 2013; Veiga and Cossart, 2006; Yamauchi and Helenius, 2013). Our data suggest that further experiments might be required to assess whether SWCNT also exploit this cellular entry mechanism. Other groups have noted the structural similarities between C-60, other fullerene-based structures and the geometry of viruses such as the rabies pathogen (Huang et al., 2012; Marsh and Helenius, 2006; Piccinotti et al., 2013; Yamauchi and Helenius, 2013), and it may be the entry mechanism for the latter that is being mimicked by SWCNT. We also note that unmodified CNT may be targeted for this clathrin-mediated endocytosis, implying that the ability of functional groups to modify this targeting may be a consideration in design of bioavailable therapeutics and conversely in decreasing the bioavailability of non-therapeutic, environmental CNT-derived materials (Battigelli et al., 2013; Firme and Bandaru, 2010).

In summary, incubation with pristine SWCNT aggregates directly suppressed mast cell pro-inflammatory responses. The ability of mast cells to respond to SWCNT included plasma membrane remodeling around the aggregates with clathrin clustering and cortical actin disruption at the contact zone. SWCNT suppressed multiple arms of the FcεR1 response including the biphasic calcium response and phosphorylation of post-receptor kinases such as syk. Mast cell responses to SWCNT should be confirmed in primary human cell systems and may then be factored into our understanding of CNT effects on human physiology, and in turn CNT may be considered as potential regulators of mast cell responses (Pescatori et al., 2013).

Acknowledgments

This work was funded by the Air Force Research Laboratories Minority Leaders Program (HT, MS, KK), the National Institutes of Health P20MD006084 (Chaminade University BRIC program), the NIH INBRE 2P20GM103466 (HT, EU), Hawaii Community Foundation Leahi Fund 13ADVC-60228 (AJS) and the NSF EPSCOR EPS-0903833 (HT). We thank Dr. Rajesh Naik, Dr. Saber Hussein and Dr. Elizabeth Maurer (Materials and Manufacturing Directorate, Air Force Research Laboratories, Wright Patterson Air Force Base, Dayton, OH), and L.L. Clarkson and Dr. L. Clarkson (Clarkson Aerospace) for their support of this project. AFRL paper clearance number 88ABW-2014-0826.

References

Ajayan PM, Charlier J, Rinzler AG. Carbon nanotubes: from macromolecules to nanotechnology. Proc Natl Acad Sci U S A. 1999; 96:14199–14200. [PubMed: 10588679]

Ali-Boucetta H, Nunes A, Sainz R, Herrero MA, Tian B, Prato M, Bianco A, Kostarelos K. Asbestos-like pathogenicity of long carbon nanotubes alleviated by chemical functionalization. Angew Chem Int Ed Engl. 2013; 52:2274–2278. [PubMed: 23319294]

Battigelli A, Menard-Moyon C, Da Ros T, Prato M, Bianco A. Endowing carbon nanotubes with biological and biomedical properties by chemical modifications. Adv Drug Deliv Rev. 2013

Bianco A, Kostarelos K, Partidos CD, Prato M. Biomedical applications of functionalised carbon nanotubes. Chem Commun (Camb). 2005:571–577. [PubMed: 15672140]

Boll W, Ohno H, Songyang Z, Rapoport I, Cantley LC, Bonifacino JS, Kirchhausen T. Sequence requirements for the recognition of tyrosine-based endocytic signals by clathrin AP-2 complexes. EMBO J. 1996; 15:5789–5795. [PubMed: 8918456]

Cui Y, Kim SN, Jones SE, Wissler LL, Naik RR, McAlpine MC. Chemical functionalization of graphene enabled by phage displayed peptides. Nano Lett. 2010; 10:4559–4565. [PubMed: 20942387]

Cui Y, Kim SN, Naik RR, McAlpine MC. Biomimetic peptide nanosensors. Acc Chem Res. 2012; 45:696–704. [PubMed: 22292890]

Cureton DK, Massol RH, Whelan SP, Kirchhausen T. The length of vesicular stomatitis virus particles dictates a need for actin assembly during clathrin-dependent endocytosis. PLoS Pathog. 2010; 6:e1001127. [PubMed: 20941355]

Dellinger A, Zhou Z, Norton SK, Lenk R, Conrad D, Kepley CL. Uptake and distribution of fullerenes in human mast cells. Nanomedicine. 2010; 6:575–582. [PubMed: 20138243]

Di Capite J, Parekh AB. CRAC channels and Ca2+ signaling in mast cells. Immunol Rev. 2009; 231:45–58. [PubMed: 19754889]

Firme CP 3rd, Bandaru PR. Toxicity issues in the application of carbon nanotubes to biological systems. Nanomedicine. 2010; 6:245–256. [PubMed: 19699321]

Galli SJ, Tsai M. Mast cells in allergy and infection: versatile effector and regulatory cells in innate and adaptive immunity. Eur J Immunol. 2010; 40:1843–1851. [PubMed: 20583030]

Huang HC, Chen CC, Chang WC, Tao MH, Huang C. Entry of hepatitis B virus into immortalized human primary hepatocytes by clathrin-dependent endocytosis. J Virol. 2012; 86:9443–9453. [PubMed: 22740403]

Jagota, A.; Lustig, SR.; Wang, S.; Wang, H. Carbon nanotube binding peptides. European Patent EP 1509390 (2006). US Patent 60/385696. 2002.

Jin H, Heller DA, Sharma R, Strano MS. Size-dependent cellular uptake and expulsion of single-walled carbon nanotubes: single particle tracking and a generic uptake model for nanoparticles. ACS Nano. 2009; 3:149–158. [PubMed: 19206261]

Katwa P, Wang X, Urankar R, Podila R, Hilderbrand S, Fick S, Rao AM, Ke PC, Wingard CJ, Brown JM. A Carbon Nanotube Toxicity Paradigm Driven by Mast Cells and the IL-33/ST2 Axis. Small. 2012; 8:2904–2912. [PubMed: 22777948]

Koyasu S, Moro K. Role of innate lymphocytes in infection and inflammation. Front Immunol. 2012; 3:101. [PubMed: 22783250]

Li X, Chen W, Zhan Q, Dai L, Sowards L, Pender M, Naik RR. Direct measurements of interactions between polypeptides and carbon nanotubes. J Phys Chem B. 2006; 110:12621–12625. [PubMed: 16800593]

Ma HT, Beaven MA. Regulators of Ca(2+) signaling in mast cells: potential targets for treatment of mast cell-related diseases? Adv Exp Med Biol. 2011; 716:62–90. [PubMed: 21713652]

Marsh M, Helenius A. Virus entry: open sesame. Cell. 2006; 124:729–740. [PubMed: 16497584]

Marshall JS. Mast-cell responses to pathogens. Nature Reviews Immunology. 2004; 4:787–799.

Moon TC, St Laurent CD, Morris KE, Marcet C, Yoshimura T, Sekar Y, Befus AD. Advances in mast cell biology: new understanding of heterogeneity and function. Mucosal Immunol. 2010; 3:111–128. [PubMed: 20043008]

Murphy FA, Schinwald A, Poland CA, Donaldson K. The mechanism of pleural inflammation by long carbon nanotubes: interaction of long fibres with macrophages stimulates them to amplify pro-inflammatory responses in mesothelial cells. Part Fibre Toxicol. 2012; 9:8. [PubMed: 22472194]

Murray AR, Kisin E, Leonard SS, Young SH, Kommineni C, Kagan VE, Castranova V, Shvedova AA. Oxidative stress and inflammatory response in dermal toxicity of single-walled carbon nanotubes. Toxicology. 2009; 257:161–171. [PubMed: 19150385]

Ohno H, Stewart J, Fournier MC, Bosshart H, Rhee I, Miyatake S, Saito T, Gallusser A, Kirchhausen T, Bonifacino JS. Interaction of tyrosine-based sorting signals with clathrin-associated proteins. Science. 1995; 269:1872–1875. [PubMed: 7569928]

Passante E, Frankish N. The RBL-2H3 cell line: its provenance and suitability as a model for the mast cell. Inflamm Res. 2009; 58:737–745. [PubMed: 19669619]

Pauly BS, Drubin DG. Clathrin: an amazing multifunctional dreamcoat? Cell Host Microbe. 2007; 2:288–290. [PubMed: 18005749]

Pelkmans L, Helenius A. Insider information: what viruses tell us about endocytosis. Curr Opin Cell Biol. 2003; 15:414–422. [PubMed: 12892781]

Pescatori M, Bedognetti D, Venturelli E, Menard-Moyon C, Bernardini C, Muresu E, Piana A, Maida G, Manetti R, Sgarrella F, Bianco A, Delogu LG. Functionalized carbon nanotubes as immunomodulator systems. Biomaterials. 2013; 34:4395–4403. [PubMed: 23507086]

Piccinotti S, Kirchhausen T, Whelan SP. Uptake of Rabies Virus into Epithelial Cells by Clathrin-Mediated Endocytosis Depends upon Actin. J Virol. 2013; 87:11637–11647. [PubMed: 23966407]

Poland CA, Duffin R, Kinloch I, Maynard A, Wallace WA, Seaton A, Stone V, Brown S, Macnee W, Donaldson K. Carbon nanotubes introduced into the abdominal cavity of mice show asbestos-like pathogenicity in a pilot study. Nat Nanotechnol. 2008; 3:423–428. [PubMed: 18654567]

Ryan JJ, Bateman HR, Stover A, Gomez G, Norton SK, Zhao W, Schwartz LB, Lenk R, Kepley CL. Fullerene nanomaterials inhibit the allergic response. J Immunol. 2007; 179:665–672. [PubMed: 17579089]

Sandig H, Bulfone-Paus S. TLR signaling in mast cells: common and unique features. Front Immunol. 2012; 3:185. [PubMed: 22783258]

Sismanopoulos N, Delivanis DA, Alysandratos KD, Angelidou A, Therianou A, Kalogeromitros D, Theoharides TC. Mast cells in allergic and inflammatory diseases. Curr Pharm Des. 2012; 18:2261–2277. [PubMed: 22390690]

Stern ST, McNeil SE. Nanotechnology safety concerns revisited. Toxicol Sci. 2008; 101:4–21. [PubMed: 17602205]

Suzuki Y, Yoshimaru T, Inoue T, Ra C. Discrete generations of intracellular hydrogen peroxide and superoxide in antigen-stimulated mast cells: reciprocal regulation of store-operated Ca2+ channel activity. Mol Immunol. 2009; 46:2200–2209. [PubMed: 19467708]

Veiga E, Cossart P. The role of clathrin-dependent endocytosis in bacterial internalization. Trends Cell Biol. 2006; 16:499–504. [PubMed: 16962776]

Wang S, Humphreys ES, Chung SY, Delduco DF, Lustig SR, Wang H, Parker KN, Rizzo NW, Subramoney S, Chiang YM, Jagota A. Peptides with selective affinity for carbon naotubes. Nature Materials. 2003; 2:196–200.

Yamauchi Y, Helenius A. Virus entry at a glance. J Cell Sci. 2013; 126:1289–1295. [PubMed: 23641066]

Yaron PN, Holt BD, Short PA, Losche M, Islam MF, Dahl KN. Single wall carbon nanotubes enter cells by endocytosis and not membrane penetration. J Nanobiotechnology. 2011; 9:45. [PubMed: 21961562]

Yoshimaru T, Suzuki Y, Matsui T, Yamashita K, Ochiai T, Yamaki M, Shimizu K. Blockade of superoxide generation prevents high-affinity immunoglobulin E receptor-mediated release of allergic mediators by rat mast cell line and human basophils. Clin Exp Allergy. 2002; 32:612–618. [PubMed: 11972610]

Highlights

- Carbon nanomaterials are emerging as important environmental toxicants
- Mast cells reside at the body's interfaces with its environment, and promote inflammatory responses to environmental challenges
- We examined model mast cell responses to SWCNT and C60-fullerenes, both of which negatively regulate antigen-mediated mast cell activation
- Carbon nanomaterials act at both the surface or after internalization in mast cells, and appear to interact with the Clathrin pathway

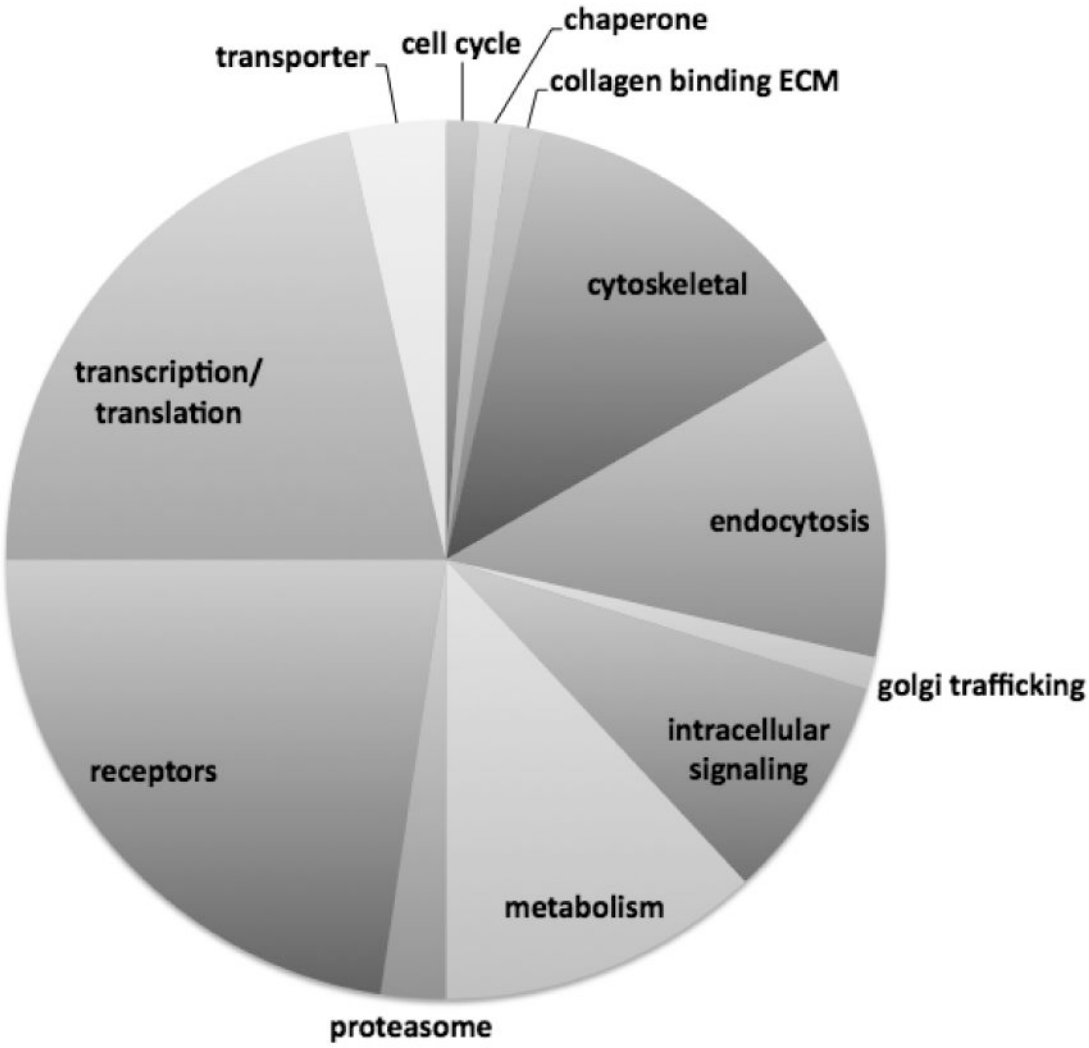

Figure 1. A. SWCNT interactome

Ten micrograms of SWCNT were used as an affinity matrix to affinity purify, in triplicate, RBL2H3 cell lysates. An irrelevant matrix was used as a negative control. Interacting protein sets (approximately 27,000 peptides) were identified using complex mixture analysis and MuDPiT (tryptase digest and LCMS/MS) at the Keck Biotechnology Facility, Yale University. Canonical groups were identified using Panther and protein groups that were over represented in the SWCNT rather than control mixtures are shown as percentage distribution within canonical groups (pie chart). Exemplar proteins for some of the groups are shown in boxes, and numbers in parentheses represent multiple occurrences of a particular protein class or type within the set of peptides over-represented in CNT affinity purifications relative to controls. **B.** Chemical characteristics of previously characterized CNT binding peptides. Peptides shown to bind directly to CNT were collated from the

literature (Wang et al., 2003, Jagota et al., 2002, 2006) and each residue from N- to C-termini was given a position number and color coded as follows: hydrophobic-aliphatic ●, hydrophobic-aromatic ●, polar neutral ●, hydroxyl or sulfur containing ●, acidic ●, basic ● and unique – cyclic ●.

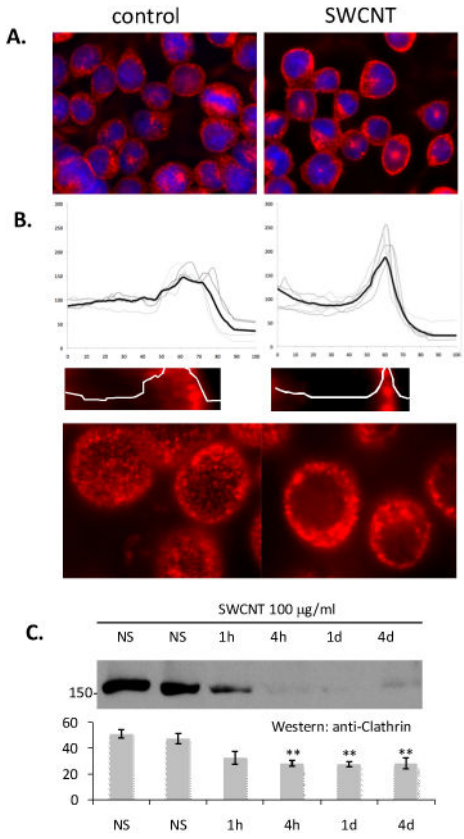

Figure 2. SWCNT cause reorganization of mast cell clathrin

A. Anti-clathrin immunofluorescence analysis was performed in RBL2H3 treated either with vehicle or 100µg/ml SWCNT for 1h. Scale bar is 20 microns. **B.** Individual (grey lines) and averaged (black line) anti-clathrin intensity profiles of 10 micron distances across the cell radius in the absence and presence of SWCNT. **C**. Example fluorescence visualizations of data in A. Scale bars are 6 microns. **D.** Western blot analysis of Clathrin expression across a timecourse of SWCNT exposure.

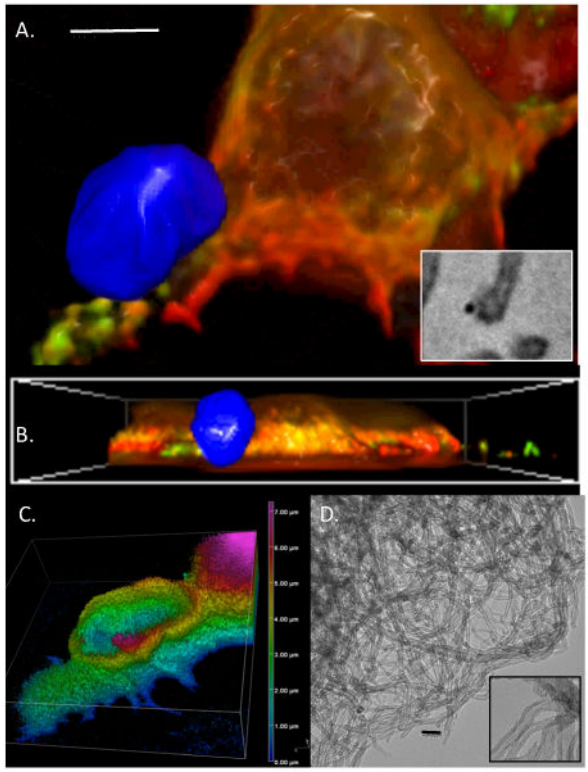

Figure 3. A-D. Membrane rearrangements in response to SWCNT aggregates in RBL2H3 cells

Plasma membrane was stained with Alexafluor 488-Wheat Germ Agglutinin (WGA) and exposed to SWCNT aggregates for 2 min. Images were taken at 10 min after exposure, an represent reconstructions **(A)** and cross-sectional **(B)** projections of epi-fluorescently imaged z stack (150 nm discs) sets digitally deconvolved and projected. SWCNT aggregate is false-colored blue. Scale bar in A is 2 microns. **A** *inset* shows SWCNT aggregate juxtaposed to an RBL2H3 cell process imaged by EM at 300,000×. Scale bar is 20nm. **C.** Z depth coding of WGA localization in immediate contact area of SWCNT aggregate. Vertical scale at right is in microns. **D.** EM partial view of SWCNT aggregate (120,000×) and individual fibrils (300,000× *inset*). Scale bar is 20nm. **E-J.** Analysis of cortical actin status in contact zone between CNT aggregate and RBL2H3 membrane. **E**. Cortical actin staining using Alexa-568 phalloidin was assessed using confocal imaging and 3D reconstruction. **F.** Deconvolved epifluorescence z stack projected using extended depth of focus projection, with contact zone between SWCNT aggregate and RBL2H3 highlighted. **G-I.** Zoomed views of control (CON, non-contact zone) and CNT contact zones (CNT) between SWCNT aggregate and RBL2H3 membrane. **J.** Intensity line scans of 1 micron sections of Alexa568-phalloidin fluorescence in G. Distance shown in arbitrary units.

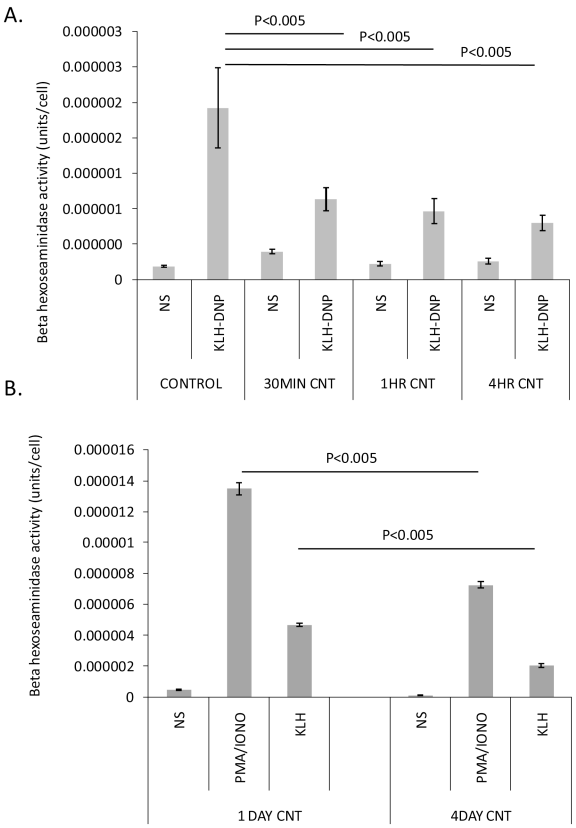

Figure 4. Suppression of mast cell secretory responses by SWCNT

Antigen (KLH-DNP) induced secretion of mast cell pro-inflammatory granules was assessed using a beta-hexoseaminidase assay. **A.** Effect of acute SWNT pre-incubation upon the intensity of antigen-induced secretory responses. **B**. Effect of 1 and 4 day chronic SWCNT exposure upon subsequent antigen-induced secretory responses.

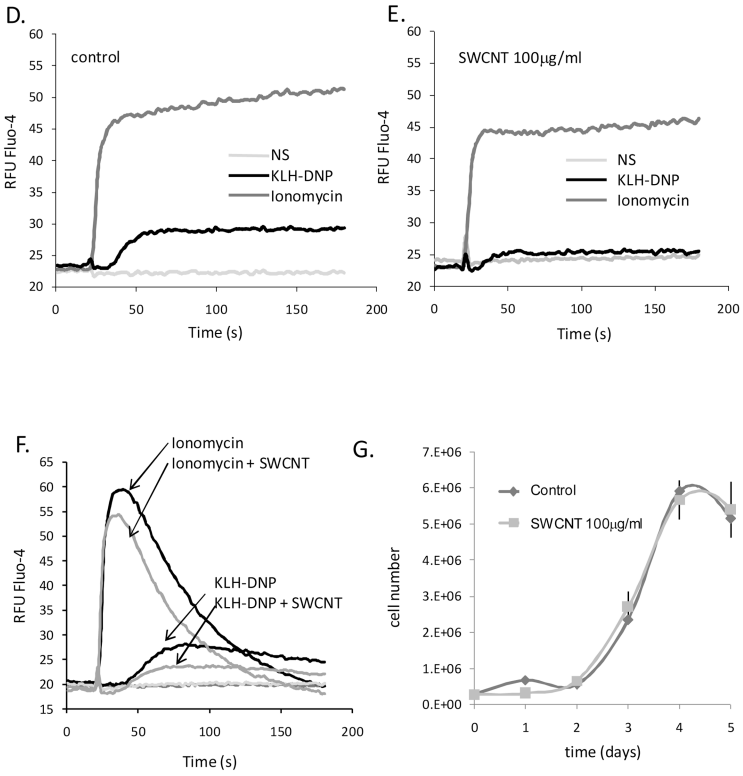

Figure 5. CNT are potent suppressors of mast cell calcium fluxes

A. *Left panel*. RBL2H3 cells were pre-incubated with 10µg/ml SWCNT for the indicated times (in days) prior to IgE loading and preparation for calcium assay. Fluo-4 loaded cells were stimulated with 200ng/ml KHL-DNP (black bar) after establishing a baseline (grey bar). *Right panel*. Area Under the Curve (AUC) analysis of calcium responses in cells pre-incubated with 100µg/ml SWCNT. AUC for 0-120s were integrated (Prism) from cells stimulated with either IgE/KLH-DNP or ionomycin after the 2-180 min pre-incubation times indicated. **B.** Dose response analysis of SWCNT effects upon ionomycin and antigen (KLH-DNP)-induced calcium responses in RBL2H3 cells. AUC of 120s calcium traces were calculated for cells stimulated as indicated with 1h pre-incubation of the indicated SWCNT doses. **C.** Comparison AUC analysis of suppression of antigen (KLH-DNP) and ionomycin induced calcium responses 0-180 min pre-incubation with 100µg/ml SWCNT. **D, E.** Matched calcium assay of control cells (D) and those pre-stimulated with 100µg/ml SWCNT for 1h (E). Indicated stimuli were added at the 20s timepoint. Experiment was performed in the presence of external calcium. **F.** Matched calcium assay of control cells and those pre-stimulated with 100µg/ml SWCNT for 1h. Indicated stimuli were added at the 20s timepoint. Experiment was performed in nominally calcium-free external medium. **G.** Growth curve of RBL2H3 incubated in the absence or presence of 100µg/ml SWCNT for the indicated time (in days).

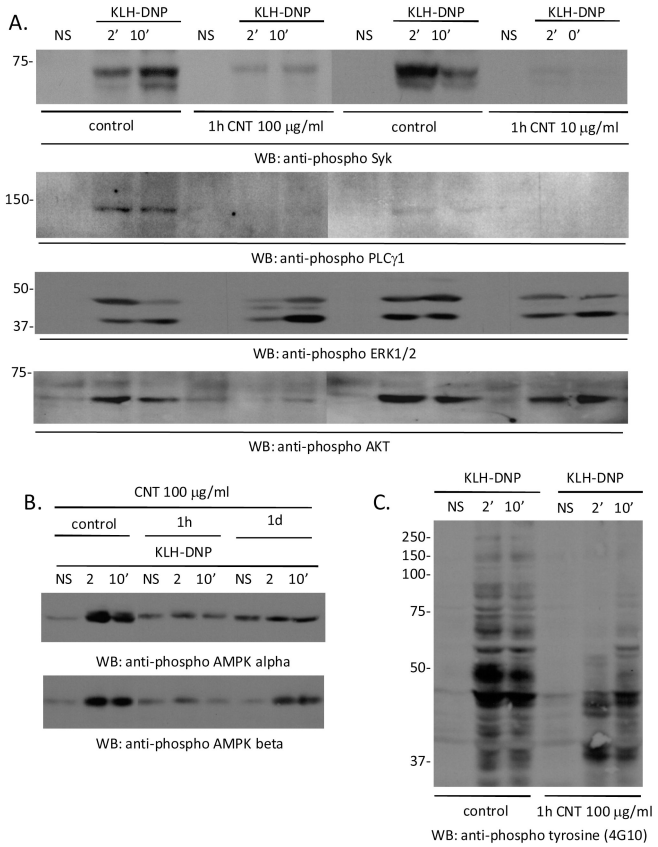

Figure 6. SWCNT suppression of membrane-proximal mast cell signaling pathways

A. We used Western blot analysis of the phosphorylation status of Syk, Phospholipase C gamma 1, and the ERK1 and ERK2 kinases. **B**. Evaluation of levels of phosphorylated AMPK kinases alpha and beta in antigen stimulated mast cells in the absence and presence of SWCNT at the indicated concentration. **C**. Evaluation of total tyrosine phosphorylation (4G10-reactive proteins) in antigen stimulated mast cells in the absence and presence of SWCNT at the indicated concentration.

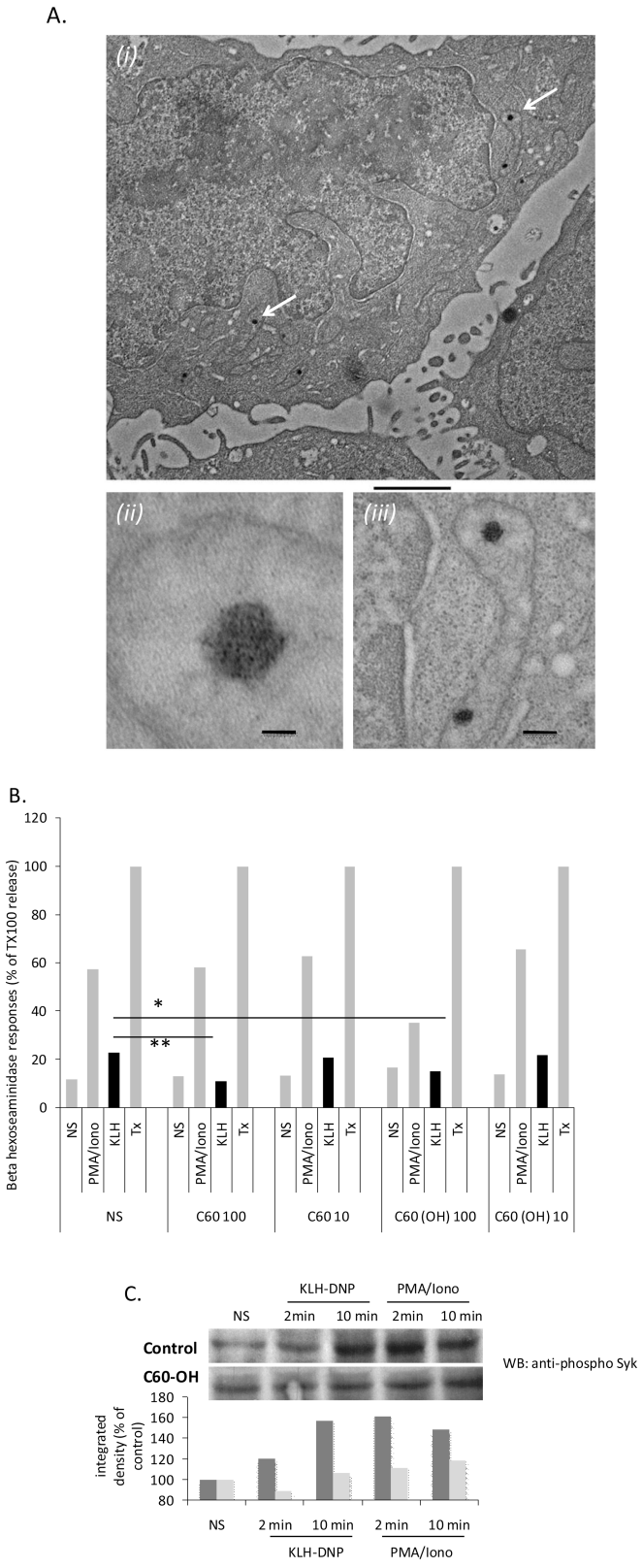

Figure 7. Pristine or hydroxylated fullerenes are suppressors of FcεRI pathways *in vitro*

A. EM analysis of RBL2H3 exposed to hydroxylated fullerenes showing internalized C60 particles. (i) 3000x image with scale bar of 2 microns. White arrows point to probable C60 particles. (ii) 100,000x image with scale bar of 20nm. (iii) 30,000x image with scale bar of 100nm. **B.** Antigen (KLH-DNP)-induced or pharmacologically (PMA/Ionomycin)-induced secretion of mast cell pro-inflammatory granules was assessed using a beta-hexoseaminidase assay. Experiments were performed on either cells not stimulated (NS) with fullerenes or exposed to the indicated doses (μg/ml) of pristine C-60 or hydroxylated C-60. Data are shown relative to Triton x100 (Tx) lysis of a duplicate cell sample (100% releasable hexoseaminidase). **C.** Anti-phospho syk Western blot of lysates from RBL2H3 stimulated with either antigen (KLH-DNP) or PMA/Ionomycin in the absence (upper) or presence (lower panel) of 100μg/ml hydroxylated C-60. Bar chart shows Western quantification. Dark and light grey bars represent pristine and hydroxylated C-60 treatments respectively,